

Scattering of two heavy Fermi polarons: resonances and quasibound states

Tilman Enns,¹ Binh Tran,² Michael Rautenberg,² Manuel Gerken,² Eleonora Lippi,²
Moritz Drescher,¹ Bing Zhu,^{2,3} Matthias Weidemüller,² and Manfred Salmhofer¹

¹*Institut für Theoretische Physik, Universität Heidelberg, 69120 Heidelberg, Germany*

²*Physikalisches Institut, Universität Heidelberg, 69120 Heidelberg, Germany*

³*Hefei National Laboratory for Physical Sciences at the Microscale and Department of Modern Physics,
and CAS Center for Excellence and Synergetic Innovation Center in Quantum Information and Quantum Physics,
University of Science and Technology of China, Hefei 230026, China*

(Dated: April 20, 2022)

Impurities in a Fermi sea, or Fermi polarons, experience a Casimir interaction induced by quantum fluctuations of the medium. When there is short-range attraction between impurities and fermions, also the induced interaction between two impurities is strongly attractive at short distance and oscillates in space for larger distances. We theoretically investigate the scattering properties and compute the scattering phase shifts and scattering lengths between two heavy impurities in an ideal Fermi gas at zero temperature. While the induced interaction between impurities is weakly attractive for weak impurity-medium interactions, we find that impurities strongly and attractively interacting with the medium exhibit resonances in the induced scattering with a sign change of the induced scattering length and even strong repulsion. These resonances occur whenever a three-body Efimov bound state appears at the continuum threshold. At energies above the continuum threshold, we find that the Efimov state in medium can turn into a quasibound state with a finite decay width.

I. INTRODUCTION

The interaction of impurity particles in a medium is studied across physical disciplines. Specifically, the Casimir interaction between two impurities arises from fluctuations of the medium, or even the vacuum, subject to the boundary conditions imposed by the impurities [1]. Current applications range from neutron stars [2] and the quark-gluon plasma [3] to ultracold atoms [4, 5]. Recent advances in experiments with ultracold atomic gases allow exploring mobile impurities in a fermionic medium, or Fermi polarons, in the regime of strong attraction [6–12] and precisely measuring their spectral properties. These experiments are performed not on a single impurity but on a dilute gas of impurities. The induced interaction between impurities is typically weak [13–16], but it can play an important role when the impurity-medium interaction becomes strong. Indeed, for large scattering length it can lead to Efimov three-body bound states [17–19] that are crucial for interpreting impurity spectra [20].

The interaction between localized spins in an electron gas is a classic result of condensed matter physics: by the Pauli principle, the induced Ruderman-Kittel-Kasuya-Yosida (RKKY) interaction oscillates in space and changes sign whenever the distance between the spins grows by about an electron spacing, or Fermi wavelength [21–23]. For larger objects in a Fermi sea, this can be understood by semiclassical methods [24]. More recently, these studies have been extended to the case of impurity atoms in a Fermi gas, or Fermi polarons [25–27]. When the impurity is tuned to strong attraction with the Fermi sea, it can form a bound state with one of the fermions [26, 28, 29]. These, in turn, lead to an enhanced attraction between two impurities at short distance [4, 5, 30]

and even to bipolaron bound states between two impurities in a Fermi sea [5, 31–34]. The Efimov bound states between two impurities and one fermion are characterized by discrete scaling relations [18, 35]. In the medium, the scaling relations are modified by the Fermi wavelength as an additional length scale [5, 31, 33, 34] and lead to shifts in the bipolaron resonance positions. Because they satisfy a new scaling relation, we shall refer to them as in-medium Efimov resonances. In the limit of a dense medium the induced interaction diminishes proportional to the Fermi wavelength and eventually vanishes [30].

In this work, we study the scattering properties of two heavy impurities in an ideal Fermi gas, as shown in Fig. 1. Based on the Casimir interaction potential [4], we compute the scattering phase shift and the induced scattering length between impurities and find that they scatter resonantly whenever an Efimov bound state appears at

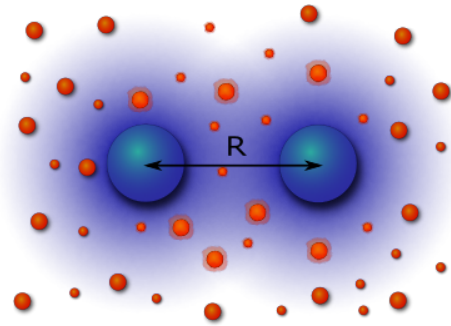


FIG. 1. Two heavy impurities (large blue dots) at distance R in a Fermi sea of light fermions (small red dots).

the continuum threshold. Moreover, for positive scattering length a repulsive barrier arises in the impurity potential, and remarkably the in-medium Efimov state can live on behind the barrier as a quasibound state at positive energies. In the following, we start by reviewing the Casimir interaction potential in Sec. II. In Section III we solve the Schrödinger equation for two impurities in this potential to find the scattering properties, and we discuss our results also for the experimentally relevant case of cesium-lithium mixtures [36, 37] before concluding in Sec. IV.

II. CASIMIR INTERACTION

The interaction of two heavy impurities (mass M) in an ideal Fermi gas of light particles (mass m) is well described in the Born-Oppenheimer approximation. By the separation of time scales, the impurities can be considered as a static scattering potential for the fermions and—in the case of a contact potential—provide only a boundary condition for the fermion wavefunctions. This approximation becomes exact in the limit of infinitely heavy impurities, where the problem reduces to potential scattering, and remains accurate at large mass ratio $M/m \gg 1$, for instance in a quantum gas mixtures of bosonic ^{133}Cs and fermionic ^6Li atoms. In this section we present the derivation of the interaction $V(R)$ induced between the two heavy impurities (of arbitrary statistics) by the presence of the Fermi sea, following Nishida [4].

Consider two infinitely heavy impurities at distance R with positions $\mathbf{R}_{1,2} = \pm\mathbf{R}/2$. The impurities have a short-range attractive interaction with the fermions, which we model by a zero-range Fermi pseudopotential. The action of the potential is equivalent to imposing the Bethe-Peierls boundary condition on the fermion wavefunction near an impurity at position \mathbf{R}_i ,

$$\psi(\mathbf{x} \rightarrow \mathbf{R}_i) \propto \frac{1}{|\mathbf{x} - \mathbf{R}_i|} - \frac{1}{a} + \mathcal{O}(|\mathbf{x} - \mathbf{R}_i|). \quad (1)$$

Here, a denotes the impurity-fermion scattering length that fully characterizes the contact interaction. The fermion wavefunctions solve the free Schrödinger equation, subject to the boundary conditions (1) at both \mathbf{R}_1 and \mathbf{R}_2 . There are potentially two bound states at negative energies $E_{\pm} = -\kappa_{\pm}^2/2m < 0$, where the inverse length scale of the bound states $\kappa_{\pm} > 0$ is given by

$$\kappa_{\pm} = \frac{1}{a} + \frac{1}{R}W(\pm e^{-R/a}) \quad (2)$$

in terms of the Lambert W function that solves $x = W(x)e^{W(x)}$. Since real solutions exist for $x \in (-1/e, \infty)$, the bound state $\kappa_{\pm} > 0$ appears for distances $R/a > \mp 1$: while κ_- exists only for positive scattering length and $R > a > 0$, κ_+ exists both for $a < 0$ at small separation $R < |a|$ and for $a > 0$ at arbitrary R . Hence, a fermion attracted to two impurities forms a κ_+ bound state much

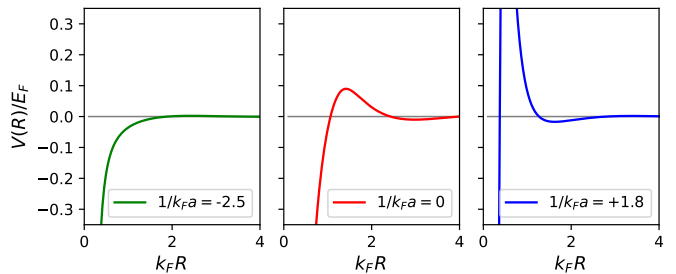


FIG. 2. Induced interaction potential $V(R)$ between two heavy impurities for negative, unitary, and positive inter-species scattering length a (from left to right). Data shown for Cs-Li mass ratio $M/m = 22.17$.

more *easily* than one attracted only to a single impurity, and this will have dramatic consequences for the scattering properties between two impurities.

Besides the bound states, there is a continuum of fermion scattering states at positive energy $E = k^2/2m > 0$. For each mode \mathbf{k} , the fermion wavefunction $\sin(kr + \delta_{\pm})$ at large distance r from both impurities acquires an s -wave phase shift with respect to the free wavefunction without impurities, which is given by

$$\tan \delta_{\pm}(k) = -\frac{kR \pm \sin(kR)}{R/a \pm \cos(kR)} \quad (3)$$

for the (anti-)symmetric solution, where $0 \leq \delta_{\pm}(k) < \pi$. In the thermodynamic limit, the total energy change with and without impurities can be expressed as

$$\Delta E(R) = -\frac{\kappa_+^2 + \kappa_-^2}{2m} - \int_0^{k_F} dk k \frac{\delta_+(k) + \delta_-(k)}{\pi m}. \quad (4)$$

At large separation the impurities no longer interact, and the energy change approaches

$$\Delta E(R \rightarrow \infty) \rightarrow 2\mu, \quad (5)$$

or twice the single-polaron energy (chemical potential)

$$\mu = -\varepsilon_F \frac{k_F a + [1 + (k_F a)^2][\pi/2 + \arctan(1/k_F a)]}{\pi(k_F a)^2} \quad (6)$$

in terms of the Fermi energy $\varepsilon_F = k_F^2/2m$. The resulting Casimir interaction relative to the chemical potential,

$$V(R) = \Delta E(R) - 2\mu, \quad (7)$$

is shown in Fig. 2. For short distance it is strongly attractive as $-c^2/2mR^2$ from the bound-state contribution κ_+ , where $c = W(1) \approx 0.567143$ solves $c = e^{-c}$; this effect is already present for a single fermion and gives rise to the Efimov effect [17–19]. In the fermionic medium, the Pauli principle requires that the induced interaction changes sign after an average spacing between the fermions, similar to the RKKY interaction in solids [21–23]. The strong attraction is thus cancelled at larger

distances by the contribution from the Fermi sea and crosses over near $k_F R \simeq 1$ into an oscillating decay $\cos(2k_F R)/R^3$ at large distance. Specifically at unitarity, the bound-state contribution $-c^2/2mR^2$ is present for *all* R and is cancelled by the Fermi-sea contribution $2\mu + c^2/2mR^2 - \cos(2k_F R)/2\pi m k_F R^3 + \mathcal{O}((k_F R)^{-4})$. For positive scattering length, a substantial repulsive barrier develops that will be able to capture a quasibound state, as we will discuss in the next section.

III. SCATTERING BETWEEN IMPURITIES

Given the induced potential $V(R)$ between the impurities, we now generalize the approach of Ref. [4] to bosonic or distinguishable impurities and compute their scattering properties in the s -wave channel. We still work in the Born-Oppenheimer approximation where the heavy impurities move slowly, while the Fermi sea of light particles adjusts almost instantaneously to their positions and produces the potential. The stationary states of the impurities are then described by the Schrödinger equation

$$\left[-\frac{\nabla_{\mathbf{R}}^2}{M} + V(R) + 2\mu - E \right] \Psi(\mathbf{R}) = 0 \quad (8)$$

in the central potential $V(R)$. The scattering properties are encoded in the scattering phase shifts $\delta_{\ell}^{\text{ind}}(k)$ induced by the medium in the ℓ partial wave component. We compute the s -wave phase shift by integrating the variable phase equation [38]

$$k \partial_R \delta_{\ell=0}^{\text{ind}}(k, R) = -MV(R) \sin[kR + \delta_{\ell=0}^{\text{ind}}(k, R)]^2. \quad (9)$$

Usually, one imposes the boundary condition $\delta_{\ell=0}^{\text{ind}}(k, R=0) = 0$ at $R=0$ and integrates up to large R , where one reads off the phase shift $\delta_{\ell=0}^{\text{ind}}(k) = \delta_{\ell=0}^{\text{ind}}(k, R \rightarrow \infty)$.

A. Efimov resonances

The short-range singularity of the induced potential $V(R \rightarrow 0) = -\alpha/R^2$ leads to a Hamiltonian that is bounded from below only for weak attraction $\alpha < 1/4$; for larger α there are an infinite number of Efimov bound states [18]. In our case $\alpha = (M/2m)c^2$ is always above $1/4$ in the Born-Oppenheimer limit $M \gg m$, so the potential needs a regularization, which is physically provided by the repulsive core of the van der Waals potential between impurities [34]. We mimic the actual potential by a hard sphere of radius R_0 , where the initial condition reads $\delta_{\ell=0}^{\text{ind}}(k, R_0) = -kR_0$, and integrate $R = R_0 \dots \infty$ using a standard ODE solver (DOP853). The cutoff radius R_0 is tuned to match the size of the lowest Efimov state in the real potential and is therefore directly related to the three-body parameter (3BP) which incorporates the relevant short-range physics [18, 39]. As a specific example, in the Cs-Li system the heteronuclear Feshbach resonance at 889 G has $a_-^{(1)} = -2130 a_B$ [40], which is

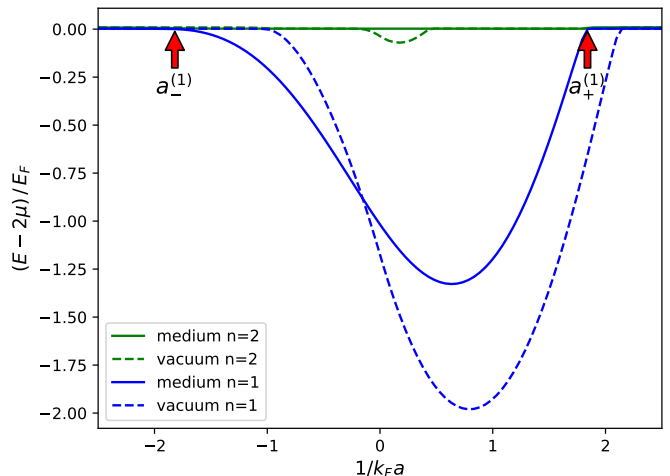


FIG. 3. Energy spectrum of Cs-Cs-Li Efimov states vs impurity-fermion scattering. The energies are given relative to the scattering continuum 2μ . Shown are the first ($n = 1$, blue (lower) lines) and second ($n = 2$, green (upper) lines) Efimov states, both in vacuum (dashed) and in medium (solid), with cutoff radius $R_0 = 0.1 k_F^{-1}$. The Efimov bound states merge with the continuum at scattering lengths $a_{\pm}^{(n)}$, as indicated by the arrows for the first in-medium Efimov state. In vacuum, length units are $10R_0$ and energy units $1/2m(10R_0)^2$.

reproduced by the induced potential with $R_0 = 220 a_B$. For a typical fermion density of $n = 10^{13} \text{ cm}^{-3}$ in current experiments [10, 15] we thus obtain $k_F R_0 = 0.1$ and we use this value in our plots to make quantitative predictions.

The bound-state spectrum for Eq. (8) is shown in Fig. 3 for the example of ^{133}Cs impurities in a ^6Li Fermi sea. One observes that the medium facilitates binding for weak attraction (shifting the onset to the left), but the repulsive barrier inhibits binding compared to the vacuum case for strong attraction [33].

B. Induced scattering length

For a given cutoff radius R_0 and the corresponding Efimov spectrum, we compute the resulting s -wave scattering phase shifts $\delta_{\ell=0}^{\text{ind}}(k)$ that are shown in Fig. 4. In the limit of small k one can read off the induced impurity-impurity scattering length a_{ind} shown in the figure and the effective range r_e from the effective range expansion

$$k \cot[\delta_{\ell=0}^{\text{ind}}(k)] = -\frac{1}{a_{\text{ind}}} + \frac{r_e}{2} k^2 + \mathcal{O}(k^4). \quad (10)$$

Equivalently, the scattering length can be obtained from the variable phase equation (9) directly in the $k \rightarrow 0$ limit,

$$\partial_R a_{\text{ind}}(R) = -MV(R)[R - a_{\text{ind}}(R)]^2, \quad (11)$$

with initial condition $a_{\text{ind}}(R_0) = R_0$ and the final result $a_{\text{ind}} = a_{\text{ind}}(R \rightarrow \infty)$. The Efimov bound states

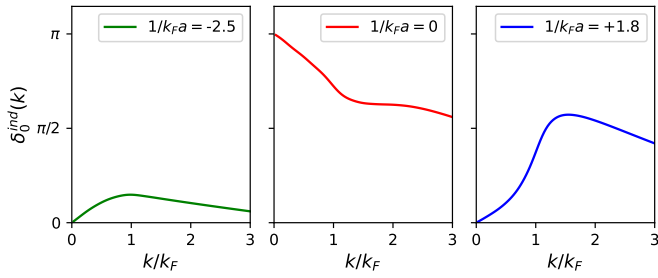


FIG. 4. Induced scattering phase shift $\delta_0^{\text{ind}}(k)$ for the potentials in Fig. 2. The initial slope near $k = 0$ determines the induced scattering lengths $k_F a_{\text{ind}} = -0.8; +0.7; -1.0$ from left to right. On the $a > 0$ side the phase shift steeply rises above $\pi/2$ indicating a quasibound state. Data shown for Cs-Li mass ratio $M/m = 22.17$.

lead to resonances in the induced scattering length [41], which are understood analytically from the solution of Eq. (11) for the $-\alpha/R^2$ potential with $\alpha > 1/4$ for distances $R_0 \dots R$,

$$a_{\text{ind}}(R) = R \left[1 - \frac{1}{2\alpha} + \frac{s_0}{\alpha} \tan \left(\arctan \frac{1}{2s_0} - s_0 \ln \frac{R}{R_0} \right) \right] \quad (12)$$

with $s_0 = \sqrt{\alpha - 1/4} > 0$ [42]. This solution is valid for distances $R_0 < R \ll |a|, k_F^{-1}$ and shows that the continuous scale invariance of the $1/R^2$ potential is broken down to a discrete scaling symmetry. The solution repeats itself whenever $s_0 \ln(R/R_0)$ is a multiple of π , hence is log-periodic in R with a length scale factor of $l = \exp(\pi/s_0)$. For the case of ^{133}Cs impurities in ^6Li , the scale factor is $l \approx 5.6$ in the Born-Oppenheimer approximation, close to the experimentally observed value of $l \approx 4.9$ [35]. For larger distance $R \gtrsim k_F^{-1}$ the $-\alpha/R^2$ form of the potential is cut off by the Fermi sea, and no Efimov bound states of size larger than k_F^{-1} occur.

The full potential $V(R)$ in Eqs. (4), (7) is computed numerically and agrees with known analytical limits for small or large distance and weak or strong coupling [4]. The induced scattering length for the full potential is shown in Fig. 5 for $k_F R_0 = 0.1$ (blue solid line). In this case, a_{ind} exhibits two scattering resonances at $a = a_{\pm}^{(1)}$, where a bound state crosses the continuum threshold. For smaller R_0 , the potential admits more bound states and associated resonances at $a = a_{\pm}^{(n)}$ with $n > 1$, for comparison see Fig. 2(b) in Ref. [33]. In the interval $1/a_-^{(n)} < 1/a < 1/a_+^{(n)}$ the induced potential admits n Efimov bound states, and the phase shift starts at $\delta_{\ell=0}^{\text{ind}}(k \rightarrow 0) = n\pi$ in accordance with Levinson's theorem, as shown for $n = 1$ in the central panel of Fig. 4.

The resonances of $a_{\text{ind}}(a)$ occur whenever an Efimov bound state crosses the continuum threshold. This can be seen in the energy spectrum in Fig. 3: for $1/a > 1/a_-^{(n)}$ the potential is deep enough to admit the n th bound state, but for even stronger attraction this bound state eventually merges again with the scattering continuum at

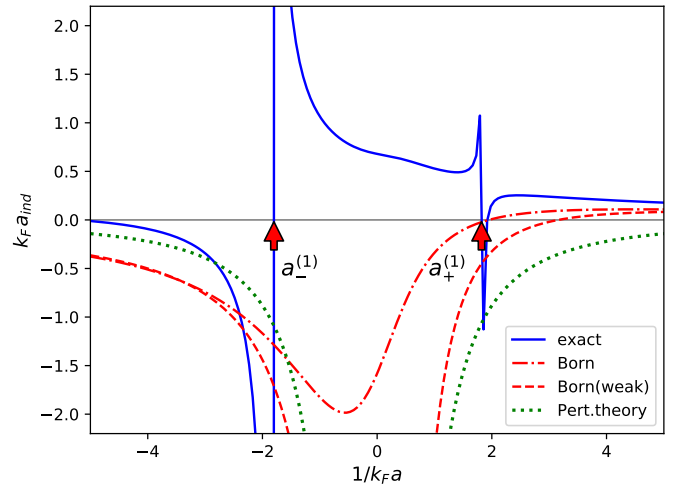


FIG. 5. Induced interaction between two heavy impurities: induced scattering length a_{ind} vs impurity-fermion interaction. From top to bottom: exact solution of Schrödinger equation (11) with cutoff $k_F R_0 = 0.1$ (blue solid line), Born approximation (13) (red dash-dotted line), analytical weak-coupling Born approximation (15) (red dashed line), and second-order perturbation theory (16) (green dotted line). The exact a_{ind} diverges at the in-medium Efimov resonances $a_{\pm}^{(1)}$ indicated by the arrows. Data shown for Cs-Li mass ratio $M/m = 22.17$.

$1/a = 1/a_+^{(n)}$. Note that the resonance positions $a_{\pm}^{(n)}(k_F)$ in medium depend on the density and differ from the vacuum values $a_{\pm}^{(n)}(0)$, as discussed in Refs. [31, 33, 34].

For the singular potential $V(R)$, the exact induced scattering length a_{ind} can differ drastically from the one obtained in Born approximation,

$$a_{\text{ind}}^{\text{Born}} = \int_0^{\infty} dR R^2 M V(R). \quad (13)$$

Here, the asymptotics at short distance [$1/R^2$] and at large distance [$\cos(2k_F R)/R^3$] are integrable and no cut-off R_0 is needed. The resulting scattering length is shown in Fig. 5 (red dash-dotted line); as might be expected for a singular potential, it does not approximate the exact solution well even for weak coupling.

It is instructive to compare the induced scattering length to the exact result in the weakly attractive limit $1/k_F a \lesssim -1$. In this case, the full induced potential is given analytically for all R as the sum of the singular attractive potential from the bound state and the regular oscillating potential from the Fermi sea,

$$V_{\text{weak}}(R) = -\frac{\Theta(|a| - R)}{2mR^2} \left(W(e^{R/|a|}) - \frac{R}{|a|} \right)^2 + \frac{a^2}{2m} \frac{2k_F R \cos(2k_F R) - \sin(2k_F R)}{2\pi R^4} + \mathcal{O}((k_F a)^3). \quad (14)$$

For weak coupling, we find an analytical expression for the induced scattering length in Born approximation

with $R_0 = 0$ [red dashed line in Fig. 5],

$$a_{\text{weak}}^{\text{Born}} = \frac{M}{2m} \left(\gamma a - \frac{k_F}{\pi} a^2 + \mathcal{O}(a^3) \right) \quad (15)$$

where $\gamma = \int_0^1 dx [W(e^x) - x]^2 = 2(1 - c[1 + c(1 + c/3)]) \approx 0.100795$. Figure 5 shows that the analytical weak-coupling form (15) agrees with the numerical Born solution (13) for $|k_F a| \lesssim 0.3$. Finally, second-order perturbation theory for weakly repulsive interaction yields [43]

$$a_{\text{ind}}^{\text{PT}} = -\frac{k_F}{2\pi} \frac{(M+m)^2}{Mm} a^2 + \mathcal{O}(a^3) \quad (16)$$

from the continuum of scattering states alone [green dotted line in Fig. 5]. This result at order $\mathcal{O}(a^2)$ fully agrees with the second-order term in the Born approximation (15) in the Born-Oppenheimer limit $M \gg m$. However, the first term in the Born approximation (15) that arises from the bound state is of *first order* in a and therefore dominates over the continuum contribution at weak coupling $R_0 < |a| \lesssim k_F^{-1}$. Hence, the usual perturbation theory for repulsive impurities is unable to describe attractive impurities even at weak coupling because it misses the leading bound-state contribution for $|a| > R_0$. In the exact solution of the Schrödinger equation, the bound-state contribution can become arbitrarily large near an Efimov resonance, depending on the value of the cutoff radius R_0 . Only for very weak attraction with $|a| \lesssim R_0$ the bound-state contribution is small, and the induced scattering is dominated by the second-order contribution (16), as is the case in Ref. [14] where $k_F a \approx -0.012$, and in Ref. [15].

C. quasibound states

Beyond the Efimov threshold $1/a > 1/a_+^{(n)}$ at positive scattering length, the in-medium Efimov bound state is pushed out of the potential to energies above the continuum threshold, but it may be caught behind the repulsive barrier that is created by the fermionic medium and the two-body bound states [right panel of Fig. 2]. How long the bound state can be caught behind the barrier depends on the effective height of the potential in the Schrödinger equation (8), which is proportional to the mass ratio M/m . The larger the mass ratio, the longer lived is the quasibound state even at positive energies. We find long-lived states approximately for $M/m \gtrsim 40$. In this case, the Efimov bound state goes over into a quasibound state at positive energies and with a small decay width, similar to the collisionally stable quasibound states found in Ref. [44]. We identify such a state when the scattering phase shift assumes the form of a Breit-Wigner resonance at positive energies $E = k^2/2m$ as shown in Fig. 6,

$$\cot[\delta_{\ell=0}^{\text{ind}}(k)] = -\frac{E - E_{\text{qbnd}}}{\Gamma_{\text{qbnd}}/2} + \dots \quad (17)$$

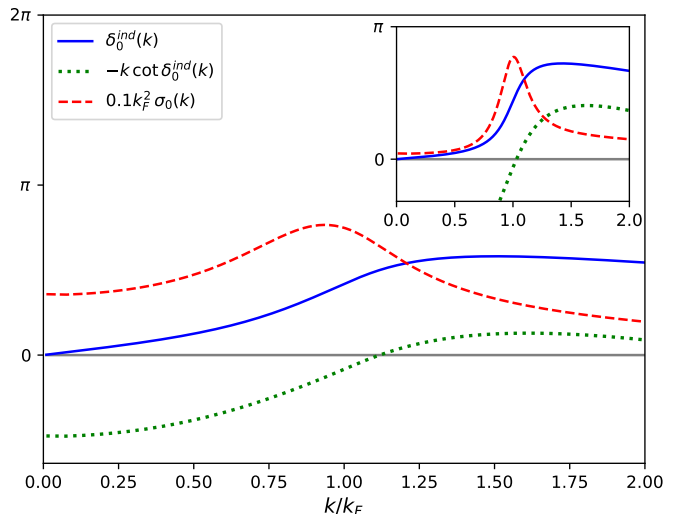


FIG. 6. Scattering resonance at positive energy above the continuum threshold and quasibound states. Enhanced scattering occurs at the upturn of the scattering phase shift $\delta_0^{\text{ind}}(k)$ (blue solid line) at $k = 1.12 k_F$, where $\cot \delta_0^{\text{ind}}(k)$ has a zero crossing (green dotted line). Correspondingly, the s -wave differential cross section σ_0 (red dashed line) exhibits a maximum at energies near ε_F . The data shown are for the Cs-Li mass ratio $M/m = 22.17$ and $k_F R_0 = 0.1$ near the Efimov resonance at $a = 0.536 k_F^{-1} \lesssim a_+^{(1)} = 0.542 k_F^{-1}$. Inset: for larger mass ratio $M/m = 44.33$ there is a well-developed scattering resonance of Breit-Wigner form (17) with $E_{\text{qbnd}} = 1.06 \varepsilon_F$ and $\Gamma_{\text{qbnd}} = 0.69 \varepsilon_F$. This arises from a quasibound state at $a = 0.359 k_F^{-1} \lesssim a_+^{(1)} = 0.360 k_F^{-1}$.

From the position of the zero crossing and the slope we read off the energy E_{qbnd} and the FWHM decay width Γ_{qbnd} . For Cs-Li parameters $M/m = 22.17$, Fig. 6 shows enhanced scattering at positive energies but still large width $\Gamma_{\text{qbnd}} > E_{\text{qbnd}}$ so that we cannot yet speak of a well-defined quasibound state. For larger mass ratio $M/m = 44.33$, we find that for $1/a > 1/a_+$ the in-medium Efimov state can turn into a well-developed quasibound state as shown in the inset: it has a decay width $\Gamma_{\text{qbnd}} < E_{\text{qbnd}}$ smaller than its energy.

Based on [19, 33], it appears reasonable to assume that the excited quasibound trimer state will eventually decay into two polarons, which form the continuum threshold for $1/a > 1/a_+$. The character of these polaron states depends on the scattering length across the polaron-to-molecule transition [26, 28, 29]. For strong binding $1/k_F a > (1/k_F a)_c \simeq 0.9$, which is the situation depicted in Fig. 3 near $a_+^{(1)}$, each impurity forms a tightly bound impurity-fermion dimer of energy μ embedded in the residual Fermi sea [19, 33]. For weaker binding $1/k_F a < (1/k_F a)_c$, instead, each impurity forms a Fermi polaron, which would describe the continuum threshold near higher-lying Efimov states $a_+^{(n>1)}$.

A quasibound state is also manifest as a peak in the

s -wave scattering cross section [red dashed line in Fig. 6]

$$\sigma_{\ell=0}(k) = \frac{4\pi}{k^2} \sin^2[\delta_{\ell=0}^{\text{ind}}(k)] \quad (18)$$

at positive energy. For a finite density of heavy impurities in thermal equilibrium with the medium at $T \simeq E_{\text{qbnd}}$ there will be enhanced scattering between the impurities, which would lead to a greater mean-field shift in the impurity spectra proportional to the impurity density.

Experimentally, the Efimov bound states in medium could be observed as a medium-density dependent shift of the three-body loss peaks associated with the Efimov trimers [33]. The quasibound state and scattering resonance at positive energies above the continuum threshold would lead to an impurity-density dependent shift in the polaron spectrum, estimated at a few percent in the case of Ref. [45], and to enhanced radiofrequency association of Efimov trimers [20] beyond $a_+^{(n)}$.

IV. CONCLUSION

The induced interaction between *attractive* impurities in a Fermi sea differs fundamentally from the RKKY interaction between nuclear spins in an electron gas, or repulsive impurities. While the continuum of scattering states yields a similar oscillating potential at large distance, the appearance of bound states implies a strong attraction at short distances. This singular $-1/R^2$ attraction gives rise to a series of three-body Efimov bound states down to the cutoff scale. Whenever a bound state crosses the continuum threshold, the induced scattering length a_{ind} exhibits resonances and changes sign. Attractive impurities can thus scatter strongly, and repulsively, in distinction to the weak induced attraction for repulsive impurities. For very weak attraction of order $k_F a \approx -0.01$, instead, our prediction for the induced scattering length is just slightly more attractive than in perturbation theory due to the additional attraction by the bound state, consistent with recent measurements [14, 15].

While the impurity-impurity-fermion Efimov bound states below the continuum threshold have been discussed earlier, we find that at positive scattering length

and large mass ratio the Efimov states can turn into quasibound states at positive energy. This corresponds to two impurities caught behind the repulsive potential barrier created by the Fermi sea: they can eventually tunnel through the barrier and escape, but as long as they are close, there is an enhanced probability to form a deeply bound state. This three-body recombination leads to a clear signature in experimental loss spectra [35–37].

Our investigation can be generalized to a dilute gas of heavy impurities, where it has been shown that the total Casimir energy is well approximated by a sum of pairwise two-body energies [4, 24]. It is then justified to apply our results to a thermal gas of impurities at temperature T , where the scattering properties are evaluated at the thermal wavevector $\lambda_T^{-1} = \sqrt{mT/2\pi}$. This leads to the prediction of an enhanced mean-field shift when $T \simeq E_{\text{qbnd}}$. Furthermore, if three impurities are all nearby it would be interesting to explore the emergence of four-body impurity-impurity-impurity-fermion bound states. For smaller mass ratio, corrections beyond the Born-Oppenheimer approximation have to be included [30, 46], in particular the scattering of trimers by the Fermi sea, which creates particle-hole excitations and alters the induced potential [5].

For the related case of impurities in a Bose-Einstein condensate, recent studies found many-body bound states of two impurities, or bipolarons, for moderately attractive interaction [45, 47–49]. It will be interesting to extend these studies to the regime of strong attraction on the molecular side of the Feshbach resonance, where the impurities have been shown to strongly deform the surrounding BEC [50, 51]. This again gives rise to an oscillating induced potential between the impurities that can be described using nonlocal Gross-Pitaevskii theory [52].

ACKNOWLEDGMENTS

We thank A. Volosniev for interesting discussions. This work is supported by the Deutsche Forschungsgemeinschaft (DFG, German Research Foundation), project-ID 273811115 (SFB1225 ISOQUANT) and under Germany's Excellence Strategy EXC2181/1-390900948 (the Heidelberg STRUCTURES Excellence Cluster). E.L. acknowledges support by the IMPRS-QD.

[1] H. B. G. Casimir, Proc. Kon. Ned. Akad. Wet. **51**, 793 (1948).
 [2] Y. Yu, A. Bulgac, and P. Magierski, Phys. Rev. Lett. **84**, 412 (2000).
 [3] G. Neergaard and J. Madsen, Phys. Rev. D **62**, 034005 (2000).
 [4] Y. Nishida, Phys. Rev. A **79**, 013629 (2009).
 [5] D. J. MacNeill and F. Zhou, Phys. Rev. Lett. **106**, 145301 (2011).

[6] A. Schirotzek, C.-H. Wu, A. Sommer, and M. W. Zwierlein, Phys. Rev. Lett. **102**, 230402 (2009).
 [7] S. Nascimbène, N. Navon, K. J. Jiang, L. Tarruell, M. Teichmann, J. McKeever, F. Chevy, and C. Salomon, Phys. Rev. Lett. **103**, 170402 (2009).
 [8] C. Kohstall, M. Zaccanti, M. Jag, A. Trenkwalder, P. Massignan, G. M. Bruun, F. Schreck, and R. Grimm, Nature (London) **485**, 615 (2012).
 [9] M. Koschorreck, D. Pertot, E. Vogt, B. Fröhlich, M. Feld,

- and M. Köhl, *Nature (London)* **485**, 619 (2012).
- [10] M. Cetina, M. Jag, R. S. Lous, I. Fritsche, J. T. M. Walraven, R. Grimm, J. Levinsen, M. M. Parish, R. Schmidt, M. Knap, and E. Demler, *Science* **354**, 96 (2016).
- [11] F. Scazza, G. Valtolina, P. Massignan, A. Recati, A. Amico, A. Burchianti, C. Fort, M. Inguscio, M. Zaccanti, and G. Roati, *Phys. Rev. Lett.* **118**, 083602 (2017).
- [12] Z. Yan, P. B. Patel, B. Mukherjee, R. J. Fletcher, J. Struck, and M. W. Zwierlein, *Phys. Rev. Lett.* **122**, 093401 (2019).
- [13] C. Mora and F. Chevy, *Phys. Rev. Lett.* **104**, 230402 (2010).
- [14] B. J. DeSalvo, K. Patel, G. Cai, and C. Chin, *Nature (London)* **568**, 61 (2019).
- [15] H. Edri, B. Raz, N. Matzliah, N. Davidson, and R. Ozeri, *Phys. Rev. Lett.* **124**, 163401 (2020).
- [16] K. Mukherjee, S. I. Mistakidis, S. Majumder, and P. Schmelcher, *arXiv:2007.02166* (2020).
- [17] V. Efimov, *Phys. Lett. B* **33**, 563 (1970).
- [18] E. Braaten and H. W. Hammer, *Phys. Rep.* **428**, 259 (2006).
- [19] P. Naidon and S. Endo, *Rep. Prog. Phys.* **80**, 056001 (2017).
- [20] T. Lompe, T. B. Ottenstein, F. Serwane, A. N. Wenz, G. Zürn, and S. Jochim, *Science* **330**, 940 (2010).
- [21] M. A. Ruderman and C. Kittel, *Phys. Rev.* **96**, 99 (1954).
- [22] T. Kasuya, *Prog. Theor. Phys.* **16**, 45 (1956).
- [23] K. Yosida, *Phys. Rev.* **106**, 893 (1957).
- [24] A. Bulgac and A. Wirzba, *Phys. Rev. Lett.* **87**, 120404 (2001).
- [25] F. Chevy, *Phys. Rev. A* **74**, 063628 (2006).
- [26] R. Schmidt and T. Enss, *Phys. Rev. A* **83**, 063620 (2011).
- [27] P. Massignan, M. Zaccanti, and G. M. Bruun, *Rep. Prog. Phys.* **77**, 034401 (2014).
- [28] M. Punk, P. T. Dumitrescu, and W. Zwerger, *Phys. Rev. A* **80**, 053605 (2009).
- [29] C. Mora and F. Chevy, *Phys. Rev. A* **80**, 033607 (2009).
- [30] S. Endo and M. Ueda, *arXiv:1309.7797* (2013).
- [31] N. G. Nygaard and N. T. Zinner, *New J. Phys.* **16**, 023026 (2014).
- [32] F. F. Bellotti, T. Frederico, M. T. Yamashita, D. V. Fedorov, A. S. Jensen, and N. T. Zinner, *New J. Phys.* **18**, 043023 (2016).
- [33] M. Sun and X. Cui, *Phys. Rev. A* **99**, 060701(R) (2019).
- [34] B. Tran, M. Rautenberg, M. Gerken, E. Lippi, B. Zhu, J. Ulmanis, M. Drescher, M. Salmhofer, T. Enss, and M. Weidemüller, *Braz. J. Phys.* (2020), 10.1007/s13538-020-00811-5.
- [35] J. Ulmanis, S. Häfner, R. Pires, E. D. Kuhnle, Y. Wang, C. H. Greene, and M. Weidemüller, *Phys. Rev. Lett.* **117**, 153201 (2016).
- [36] R. Pires, J. Ulmanis, S. Häfner, M. Repp, A. Arias, E. D. Kuhnle, and M. Weidemüller, *Phys. Rev. Lett.* **112**, 250404 (2014).
- [37] S.-K. Tung, K. Jimenez-Garcia, J. Johansen, C. V. Parker, and C. Chin, *Phys. Rev. Lett.* **113**, 240402 (2014).
- [38] F. Calogero, *Variable Phase Approach to Potential Scattering* (Academic Press, New York, 1967).
- [39] Y. Wang, J. Wang, J. P. D’Incao, and C. H. Greene, *Phys. Rev. Lett.* **109**, 243201 (2012).
- [40] S. Häfner, J. Ulmanis, E. D. Kuhnle, Y. Wang, C. H. Greene, and M. Weidemüller, *Phys. Rev. A* **95**, 062708 (2017).
- [41] S. Endo, P. Naidon, and M. Ueda, *Few-Body Syst.* **51**, 207 (2011).
- [42] S. Moroz, *Ann. Phys. (N.Y.)* **326**, 1368 (2011).
- [43] D. H. Santamore and E. Timmermans, *Phys. Rev. A* **78**, 013619 (2008).
- [44] O. I. Kartavtsev and A. V. Malykh, *J. Phys. B: At. Mol. Opt. Phys.* **40**, 1429 (2007).
- [45] P. Naidon, *J. Phys. Soc. Japan* **87**, 043002 (2018).
- [46] M. Schecter and A. Kamenev, *Phys. Rev. Lett.* **112**, 155301 (2014).
- [47] N. T. Zinner, *Europhys. Lett.* **101**, 60009 (2013).
- [48] A. Camacho-Guardian, L. A. Peña Ardila, T. Pohl, and G. M. Bruun, *Phys. Rev. Lett.* **121**, 013401 (2018).
- [49] A. Camacho-Guardian and G. M. Bruun, *Phys. Rev. X* **8**, 031042 (2018).
- [50] M. Drescher, M. Salmhofer, and T. Enss, *Phys. Rev. A* **99**, 023601 (2019).
- [51] M. Drescher, M. Salmhofer, and T. Enss, *arXiv:2011.06385* (2020).
- [52] M. Drescher, M. Salmhofer, and T. Enss, *Phys. Rev. Research* **2**, 032011(R) (2020).